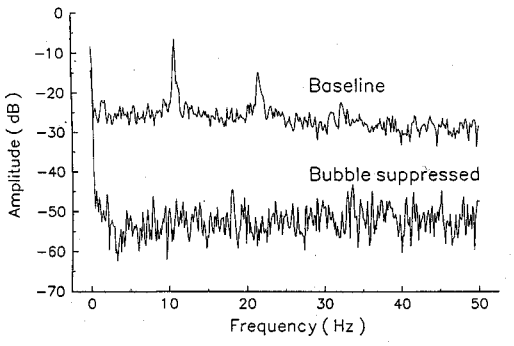

Fig. 4 Wake velocity spectra with and without the leading-edge bubble present (frequency ± 0.125 Hz and amplitude ± 0.1 dB).

inspection of these photos, aided by the surface oil flow visualization experiments, reveals the presence of the separation bubble near the leading edge. The bubble is relatively small in the top photo. By the third photo it has grown substantially and appears to have burst in the fourth. The bursting is accompanied by a complete separation of the flow and the appearance of a stall-vortex-type structure on the upper surface. The sequence of events described in the foregoing qualitatively agrees with the computational as well as experimental results presented in Ref. 2.

Figures 2 and 3 suggest that the low-frequency oscillation is related to the occurrence of the leading-edge separation bubble. This idea is supported by the data shown in Fig. 4. Wake velocity spectra at $\alpha = 15$ and $Re = 0.8 \times 10^6$ are shown with and without "zig-zag" tape placed near the leading edge. In the upper trace an oscillation frequency of 11 Hz and its first harmonic are clearly seen. In the second trace the bubble was eliminated by the zig-zag tape, which acts as both boundary-layer trip and vortex generators.[7] Not only are the low-frequency oscillation peaks gone, but also the overall energy in the wake was reduced by 30 dB. No evidence was seen of the low-frequency oscillation over the entire α range with the zig-zag tape in place and the bubble eliminated.

The unsteady behavior of separation bubbles is well known.[8–10] When nondimensionalized by the bubble length, the characteristic oscillation frequency typically corresponds to a Strouhal number of about 0.6. However, much lower frequency unsteadiness has also been reported in several references. For example, Driver et al.[9] also documented an unsteady phenomenon in their backward-facing step flow at frequencies less than 1/6th the characteristic frequency. This phenomenon, referred to as shear layer flapping, involved a momentary disorder of the shear layer where a vortex was shed, the bubble collapsed and then grew in size until another vortex was shed. This was characterized by large changes in the reattachment location and a corresponding vertical motion of the shear layer. The frequency and the flow characteristics of the phenomena considered in the present study appear to agree with those of shear layer flapping. The flow oscillation in the present case, however, is much more pronounced and symptomatic of a resonance. What completes a possible feedback loop to produce the resonance-like oscillation remains unclear and is the subject of the ongoing investigation.

Acknowledgment

The authors at the University of Illinois were supported in part by Grant NAG 3-1374 from NASA Lewis Research Center.

References

[1]Zaman, K. B. M. Q., Bar-Sever, A., and Mangalam, S. M., "Effect of Acoustic Excitation on the Flow over a Low-*Re* Airfoil," *Journal of Fluid Mechanics*, Vol. 182, 1987, pp. 127–148.

[2]Zaman, K. B. M. Q., McKinzie, D. J., and Rumsey, C. L., "A Natural Low-Frequency Oscillation of the Flow over an Airfoil near Stalling Conditions," *Journal of Fluid Mechanics*, Vol. 202, 1989, pp. 403–422.

[3]Bragg, M. B., Heinrich, D. C., and Khodadoust, A., "Low-Frequency Oscillation over Airfoils near Stall," *AIAA Journal*, Vol. 31, No. 7, 1993, pp. 1341–1343.

[4]Bragg, M. B., and Khodadoust, A., "Experimental Measurements in a Large Separation Bubble due to a Simulated Glaze Ice Accretion," AIAA Paper 88-0116, Jan. 1988.

[5]Reda, D. C., "Observations of Dynamic Stall Phenomena Using Liquid Crystal Coatings," *AIAA Journal*, Vol. 29, No. 2, 1991, pp. 308–310.

[6]Bragg, M. B., Heinrich, D. C., and Zaman, K. B. M. Q., "Flow Oscillation over Airfoils near Stall," *Proceedings of the 19th Congress of the International Council of the Aeronautical Sciences* (Anaheim, CA), Vol. 2, 1994, pp. 1639–1648.

[7]Balow, F. A., "Effect of an Unsteady Laminar Separation Bubble on the Flowfield over an Airfoil Near Stall," M.S. Thesis, Univ. of Illinois at Urbana–Champaign, IL, 1994.

[8]Pauley, L. L., Moin, P., and Reynolds, W. C., "The Structure of Two-Dimensional Separation," *Journal of Fluid Mechanics*, Vol. 220, 1990, pp. 397–411.

[9]Driver, D. M., Seegmiller, H. L., and Marvin, J., "Unsteady Behavior of a Reattaching Shear Layer," AIAA Paper 83-1712, 1983.

[10]Simpson, R. L., "Two-Dimensional Turbulent Separated Flow," AGARD, AGARDOGRAPH 287, June 1985.

Use of Drag Probe in Supersonic Flow

J. C. Richard* and G. C. Fralick†
NASA Lewis Research Center, Cleveland, Ohio 44135

I. Introduction

THE purpose of this research was to develop an instrument that could provide dynamic flow parameters in supersonic propulsion research.[1] The parameters of interest are the velocity, velocity head, Mach number, and mass flow rate.

The drag probe functions by measuring the drag on a flat cantilever beam exposed transversely to a flowfield.[2–5] This process is shown schematically in Fig. 1. The drag is measured indirectly with strain gauges attached on opposite sides of the beam's base—a layout that makes the probe inherently temperature compensated. The frequency response of the probe can be extended to 100 kHz, which rivals the frequency response of hot wires, yet it is rugged enough to survive the harsh environments often encountered in aerospace applications. Its associated electronics are as simple as those of strain-gauge pressure transducers, and it is easy to calibrate. It gives the velocity-head measurement directly and yields the velocity readily.

Use of the drag-force anemometer has been limited to subsonic-flow applications. Such use and the anemometer design are discussed by Krause and Fralick.[2] The drag force induced by the flow impinging on the probe's cantilever beam may be found from fluid-mechanics principles.[6] The coefficient of the drag imparted to the plate, C_D, has been characterized[6] as being affected by flow parameters such as the Reynolds number Re and the Mach number M. This Note focuses on demonstrating that the relation between a subsonic and a supersonic velocity head are the same for each drag probe. The supersonic flow impinging on the drag probe is assumed to be unidirectional. Krause and Fralick[2] have analyzed drag probes for the purpose of determining the flow direction. The shock region directly in front of the drag probe is assumed to be normal and two dimensional, as verified by photographs.

II. Analysis

In a supersonic flow, the force sensed by the drag probe is proportional to $(\rho u^2)_2/2$. The drag probe still senses the subsonic conditions immediately surrounding it and not the supersonic conditions

Received Sept. 6, 1994; revision received Sept. 27, 1995; accepted for publication Oct. 13, 1995.

*Aerospace Engineer, Instrumentation and Control Technology Division.
†Electrical Engineer, Instrumentation and Control Technology Division.

upstream of the shock. However, the upstream conditions are easily deduced from normal shock relations[7]:

$$M_1 = \sqrt{\frac{(\gamma+1)\left[(\rho_2 u_2^2)/(\gamma p_1)\right]-2}{\gamma-1}} \quad (1)$$

$$(\rho u^2/2)_1 = [(\gamma-1)/(\gamma+1)](\rho u^2/2)_2 + [\gamma/(\gamma+1)]p_2 \quad (2)$$

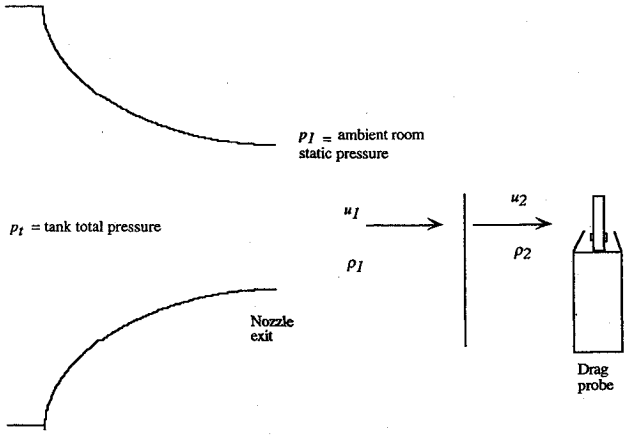

Fig. 1 Drag probe test setup. Supersonic test uses a smaller convergent–divergent nozzle, and the shock front appears when the flow is supersonic.

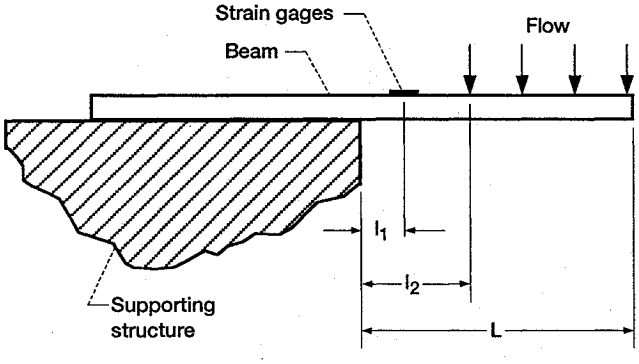

Fig. 2 Drag-probe design.[1]

Equations (1) and (2) extend the usefulness of the drag probe to the supersonic realm by permitting the computation of supersonic parameters in terms of the subsonic measurements of the drag probe. Furthermore, Eqs. (1) and (2) allow the subsonic calibration to be extended into the supersonic regime.

III. Test Program

A stainless-steel drag probe mounted on a 0.25-in.-o.d. (0.635-cm-o.d.) tube was used for testing (Figs. 1 and 2). Approximately 0.0625 in. (0.159 cm) of the active element of the drag probe protruded into the standard air-flowfield for the measurements. The distance between a strain gauge and the tip of the cantilever beam was 0.19 in. (0.48 cm). The beam was 0.1 in. (0.25 cm) wide and 0.0156 in. (0.0396 cm) thick.

Schlieren photographs of the shock structure around the drag probe were taken in a 5×5 in. (12.7×12.7 cm) wind tunnel capable of velocities from Mach 1.75–3.1. A free jet was used for subsonic measurements up to a near-sonic flow (Mach 0.9) for calibrating the drag probe.[8] A third test cell with a 1-in. (2.54-cm) exit-area supersonic nozzle on a 125-psi (0.86-MPa) line was used for subsonic testing and also for supersonic testing up to Mach 1.6 (see Fig. 1). This cell was primarily used to take images of the shock to ensure that the shock shape satisfied the normal shock assumption, but it was also used to take supersonic data. These images, produced with laser-shadowgraph techniques and a 35-mm still video camera, are discussed below.

The flow quality for the free jet has been measured, and we found that, on the centerline of the jet, the total pressure is within 1 in. (2.54 cm) of the water pressure of the tank for as far as four diameters away from the jet exit. There are insufficient data to determine the flow quality of the 125-psi (0.86-MPa) and 5×5 in. (12.7×12.7 cm) jets, but there is good agreement in the regions where the data overlap.

IV. Test Results

Results of the experiment are shown in Figs. 3–5. The subsonic calibration curve shown in Fig. 3 is similar to that reported for previous drag probes.[2,3] The slope of the curve here is roughly 2.42 psi/mV (0.0167 MPa/mV). The maximum error noted in the test cells was 2% in that the median of the subsonic portions of the tests are that close to each other. The standard deviations of these subsets of the data taken are also similar. There is a slight curvature in the transonic regime, which is known for its nonlinearity.[6]

The velocity head behind the shock follows a slope that is different from that from the subsonic portion. However, Eq. (2) indicates that there is a relation between the velocity head measured by the

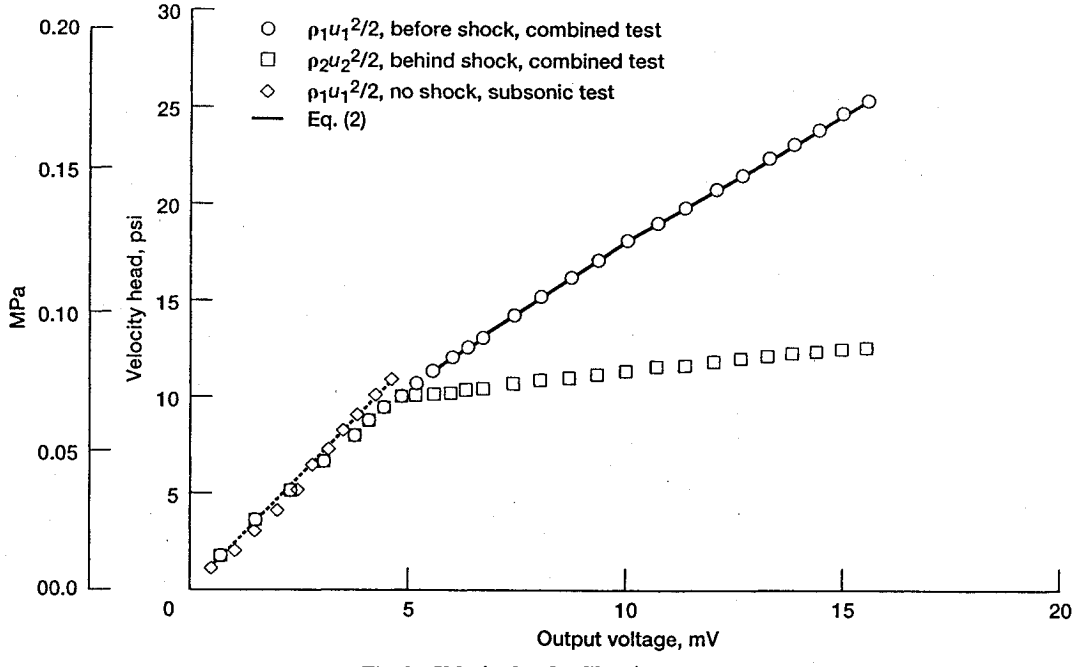

Fig. 3 Velocity-head-calibration curve.

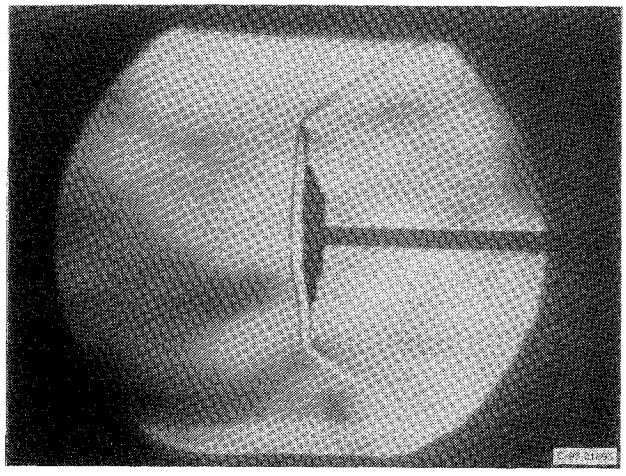

Fig. 4 Schlieren pictures of dummy (no electronics) drag probes (Mach 2).

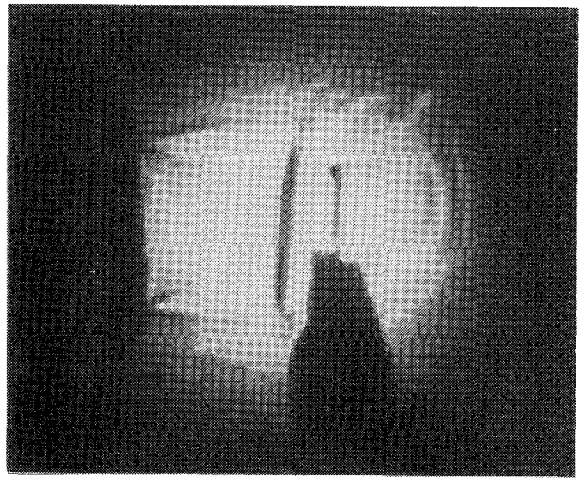

Fig. 5 Laser shadowgraphs of drag probe (Mach 2).

probe and the freestream velocity head. In fact, the results from the two sets of tests demonstrate that it is not necessary to calibrate the drag probe in a supersonic flow; subsonic calibration is sufficient. To test whether the extrapolation of the subsonic calibration into the supersonic regime derived before was valid, we tested the probe in a small jet facility that was capable of both subsonic and supersonic flows. The velocity head calculated from the other sensors' data (room and line pressures and room temperature), was plotted. Equation (2) was also plotted and is seen to be very accurate, showing that the subsonic calibration of the drag probe is adequate. The standard deviation between the two calibrations is 0.5813.

Dummy drag probes were also tested in the 5 × 5 in. (12.7 × 12.7 cm) supersonic facility to obtain schlieren images of the shock structure around the drag probe. The image shown in Fig. 4 seems to support the assumption that the shock in front of the drag probe is indeed a normal shock. The laser shadowgraphs from the combined subsonic and supersonic tests confirm a normal shock as well.

The differences between Figs. 4 and 5 with respect to the shock shape located away from the center of the probe element (the beam) as seen in the laser shadowgraphs and in the schlieren photographs are largely due to the jet from the small 1-in. nozzle vs the core flow in the larger 5 × 5 in. (12.7 × 12.7 cm) test section. The velocity profile of the jet was still tracing out a parabolic shape with the small nozzle, whereas the velocity profile in the larger test section was largely flat in the core where the probes were placed. This difference does not affect the results because the small probe element is mostly covered by the normal shock, as Figs. 4 and 5 show.

V. Conclusions

The drag-force anemometer, or drag probe, can be most useful in supersonic- as well as subsonic-flow regimes. Furthermore, a normal-shock relation between the subsonic and supersonic drag-probe results has been established. This relation indicates that a subsonically calibrated drag probe is supersonically calibrated as well.

References

[1]Cole, G. L., and Richard, J. C., "Supersonic Propulsion Simulation by Incorporating Component Models in the LArge Perturbation INlet (LAPIN) Computer Code," NASA TM 105193, Dec. 1991.

[2]Krause, L. N., and Fralick, G. C., "Miniature Drag-Force Anemometer," NASA TM Rept. X-3507, June 1977.

[3]Krause, L. N., and Fralick, G. C., "Miniature Drag-Force Anemometers," *Instrument Society of America Transactions*, Vol. 21, No. 1, 1982, pp. 117–130.

[4]Fralick, G. C., "Extending the Frequency of Response of Lightly Damped Second Order Systems: Application to the Drag Force Anemometer," NASA TM 82927, Aug. 1982.

[5]Krause, L. N., and Fralick, G. C., "Some Dynamic and Time-Averaged Flow Measurements in a Turbine Rig," *Journal of Engineering for Power*, Vol. 102, No. 1, 1980, pp. 223, 224.

[6]Hoerner, S. F., *Fluid Dynamic Drag; Practical Information on Aerodynamic Drag and Hydrodynamic Resistance*, 1965, pp. 3–14 (published by the author).

[7]Ames Research Staff, "Equations, Tables and Charts for Compressible Flow," NACA Rept. 1135, NASA Ames–Dryden Flight Research, 1953.

[8]Gettelman, C. G., and Krause, L. N., "Characteristics of a Wedge with Various Holder Configurations for Static Pressure Measurements in Subsonic Gas Streams," NACA RM E51G09, Sept. 1951

Mass Spectrometer Measurements of Test Gas Composition in a Shock Tunnel

K. A. Skinner* and R. J. Stalker†
University of Queensland,
Brisbane 4072, Queensland, Australia

Introduction

SHOCK tunnels afford a means of generating hypersonic flow at high stagnation enthalpies, but they have the disadvantage that thermochemical effects make the composition of the test flow different to that of ambient air. The composition can be predicted by numerical calculations of the nozzle flow expansion, using simplified thermochemical models, and in the absence of experimental measurements, it has been necessary to accept the results given by these calculations.

This Note reports measurements of test gas composition, at stagnation enthalpies up to 12.5 $MJkg^{-1}$, taken with a time-of-flight mass spectrometer. Limited results have been obtained in previous measurements.[1] These were taken at higher stagnation enthalpies and used a quadruple mass spectrometer. The time-of-flight method was preferred here because it enabled a number of complete mass spectra to be obtained in each test, and because it gives good mass resolution over the range of interest with air (up to 50 amu).

Experiments

The experiments were conducted in the free piston shock tunnel T4 at the University of Queensland,[2] using a helium-argon mixture as driver gas. The shock tube, of 10-m length and 75-mm diam, was operated in the shock-reflected mode and supplied shock-heated air to a contoured hypersonic nozzle with a throat diameter of 25.4 mm and an exit diameter of 261 mm. As shown in Fig. 1a, the mass

Received Feb. 24, 1995; revision received June 16, 1995; accepted for publication July 6, 1995.

*Postgraduate Student, Department of Mechanical Engineering.

†Emeritus Professor of Space Engineering, Department of Mechanical Engineering. Associate Fellow AIAA.